

Journal of Biomedical Optics

SPIEDigitalLibrary.org/jbo

Monitoring of tumor response to cisplatin by subsurface fluorescence molecular tomography

Fei Liu
Xu Cao
Wei He
Jinping Song
Zhongquan Dai
Bin Zhang
Jianwen Luo
Yinghui Li
Jing Bai

Monitoring of tumor response to cisplatin by subsurface fluorescence molecular tomography

Fei Liu,^a Xu Cao,^a Wei He,^a Jinping Song,^b Zhongquan Dai,^b Bin Zhang,^a Jianwen Luo,^{a,c} Yinghui Li,^b and Jing Bai^a

^aTsinghua University, Department of Biomedical Engineering, Beijing, 100084, China

^bChina Astronaut Research and Training Center, State Key Lab of Space Medicine Fundamentals and Application, Beijing, 100094, China

^cTsinghua University, Center for Biomedical Imaging Research, Beijing, 100084, China

Abstract. Subsurface fluorescence molecular tomography (FMT) has promising potential for noninvasive characterization of molecular and cellular activities in small animals by tomographic means in reflectance geometry. In this work, subsurface FMT is employed to monitor the therapeutic response of cisplatin in tumor-bearing mice *in vivo*. The localization and quantification accuracy of subsurface FMT are demonstrated in phantom. In the *in vivo* study, the red fluorescent protein activities not only on the surface but in the interior tumor are tracked three-dimensionally during the antitumor treatment. © 2012 Society of Photo-Optical Instrumentation Engineers (SPIE). [DOI: 10.1117/1.JBO.17.4.040504]

Keywords: fluorescence molecular tomography; reflection; reconstruction; therapeutic response.

Paper 11792L received Dec. 27, 2011; revised manuscript received Feb. 25, 2012; accepted for publication Feb. 28, 2012; published online Apr. 6, 2012; corrected Apr. 20, 2012.

Fluorescence molecular imaging has been widely applied to serve as a noninvasive, high-sensitive modality for functional and metabolic imaging in small animals *in vivo*. Fluorescence imaging in an epi-illumination geometry, also known as fluorescence reflection imaging (FRI), shines light onto tissue surface and collects emitted light from the same side of the tissue.¹ As a common technique, FRI has been widely applied in the imaging of disease pathogenesis and therapeutic response.²⁻⁴ In these studies, a topological map of the fluorescence intensity is created at the surface of the specimen. However, planar images obtained in FRI are difficult to interpret because the information they convey is surface weighted.⁵ Besides, depth information is lost because of a simple projection view in planar imaging.⁶

In order to overcome these problems, subsurface fluorescence molecular tomography (FMT) has become a promising alternative method. It is also conducted in the epi-illumination geometry, but three-dimensional (3-D) distribution of fluorochrome in the interior of tissue can be obtained by boundary

measurements and corresponding model-based tomographic reconstruction algorithms. Subsurface FMT has been investigated in phantom studies,⁷ and recently in biological tissues *ex vivo*.⁸

The stable expression of red fluorescent protein (RFP) in cancer cells can serve as an effective cell marker. The chemotherapeutic agent, cisplatin, is a widely used anticancer drug exerting its toxicity generally through induction of apoptosis. In this study, subsurface FMT is employed *in vivo*, to monitor tumor response to cisplatin by serial, noninvasive assessing of the 3-D distribution and fluorescence intensity of RFP in mouse tumor models. Here, subsurface FMT is conducted on a homemade noncontact full-angle FMT system. Considering that the distances for most sources and detectors are comparable or below the scattering length of the tissue, third-order simplified spherical harmonics (SP₃, Ref. 9) is employed to solve the forward problem in subsurface FMT reconstruction. Phantom experiments are first carried out to demonstrate the localization and quantification accuracy of the proposed method. Then the therapeutic response to cisplatin in a mouse tumor model is monitored.

The sketch of the noncontact full-angle subsurface FMT system is shown in Fig. 1. A 300-W Xenon lamp (i) (Asahi Spectra, Torrance, CA, USA) equipped with two broad-beam illumination fibers (ii) is employed to generate approximately uniform epi-illumination. Full-angle measurements are implemented by a 360 deg rotation stage (iii) working under a step-by-step mode. Signal acquisition is performed by a charge-coupled device (CCD) camera (iv) (iXon DU-897, Andor Technologies, Belfast, Northern Ireland) coupled with a 35-mm *f*/1.6 lens (v) (C3514-M, Pentax, Japan). Corresponding excitation filter (vi) and emission filter (vii) pairs are employed for data acquisition.

Subsurface FMT reconstruction was conducted on a model-based reconstruction algorithm. The fluorescent measurement $\Phi(s, r_d)$ detected at location r_d due to an area illumination $A(s)$ can be formulated as follows:¹⁰

$$\Phi(s, r_d) = \Theta \int G_{A(s)}(r)x(r)G(r_d, r)d^3r, \quad (1)$$

where $G_{A(s)}(r)$ and $G(r_d, r)$ are the Green's functions of excitation and emission light, respectively, which are the solutions of SP₃ with a corresponding boundary condition⁹ to describe the light transportation field in tissue. The optical properties are assumed equal for both excitation and emission wavelengths. Θ is a unit-less constant taking account of the unknown gain and attenuation factors of the system. $x(r)$ is the distribution of fluorescent targets at location r , which is proportional to fluorochrome concentration.

After the imaged object is discretized, a finite element solution of SP₃ is substituted into Eq. (1) and a linear equation can be constructed as follows:

$$\Phi = WX, \quad (2)$$

where X is a column vector representing the concentration of fluorescent targets to be reconstructed and W is the weight matrix.

Address all correspondence to: Jing Bai, Tsinghua University, Department of Biomedical Engineering, Beijing, 100084, China; Tel: 86-10-62786480; E-mail: deabj@tsinghua.edu.cn.

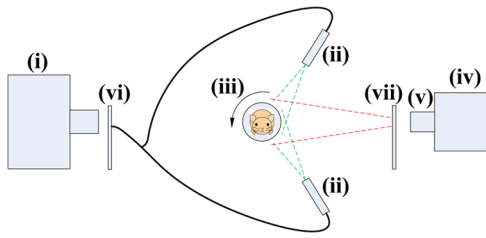


Fig. 1 Schematic top view of the noncontact full-angle subsurface FMT system.

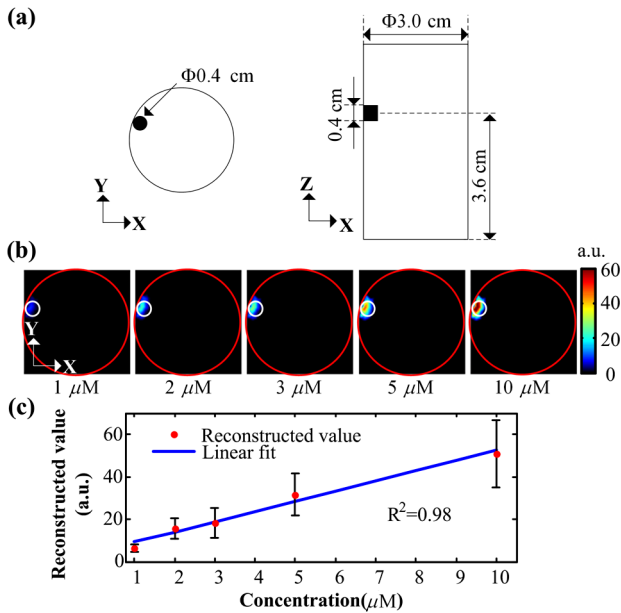


Fig. 2 Phantom experiments for evaluating the reconstruction accuracy of the system. (a) The top view and front view of the experimental configuration. (b) The reconstructed cross-section images corresponding to different ICG concentrations, respectively, taken at slice $Z = 3.6$ cm. The red curves on the cross-section images represent the phantom boundary, and the small white circles indicate the actual position of the tube. (c) Reconstructed values as a function of actual ICG concentrations. Columns, mean of the reconstructed values; bars, \pm SD. Blue solid line, linear fit ($R^2 = 0.98$).

Considering the ill-posed nature of the reconstruction, a Tikhonov regularization solution of Eq. (2) with regularization parameter of $\alpha = 10^{-2} \text{tr}(WW^T)$ is obtained from:

$$X = W^T(WW^T + \alpha I)^{-1}\Phi. \quad (3)$$

Phantom experiments were first performed to evaluate the performance of the subsurface FMT method. The phantom configuration is shown in Fig. 2(a). A 3.0-cm-diameter glass cylinder containing a mixture of water, intralipid and ink was employed as the phantom, with an absorption coefficient of $\mu_a = 0.3 \text{cm}^{-1}$ and a reduced scattering coefficient of $\mu'_s = 10.0 \text{cm}^{-1}$. A transparent glass tube (0.4 cm in diameter, 0.4 cm in length) was placed directly against the edge of the cylinder with no gap between them to simulate a subsurface distribution of the fluorescent target. The tube was sequentially filled with different concentrations of indocyanine green (ICG) and corresponding fluorescence datasets were acquired subsequently. In the phantom study, fluorescent images were acquired with a $740 \pm 6 \text{nm}$ excitation filter and a $840 \pm 6 \text{nm}$ emission filter. Background images were acquired with a $660 \pm 6 \text{nm}$ excitation filter for background signal reduction.¹¹ 72 white-light images were collected to recover the 3-D surface of the phantom.¹²

Figure 2(b) shows five cross-section slices taken at the middle of the tube ($Z = 3.6$ cm). Reconstructed values were plotted as a function of actual ICG concentrations, as depicted in Fig. 2(c). The data demonstrates that the proposed method provides a good linear response from 1 to 10 μM of the fluorescent marker. It can be seen from Figs. 2(b) and (c) that all tubes with different concentrations of ICG can be correctly localized and quantified.

Animal experiments were conducted under the protocol approved by the Institutional Animal Care and Use Committee of Tsinghua University. 1×10^6 DsRed expressing MDA-MB-231 human breast carcinoma cells were injected subcutaneously into the back of two BALB/c-nude mice (five weeks old), respectively, and treatment was initiated on day 16. One tumor-bearing mouse was administered cisplatin (1.0 mg/kg)

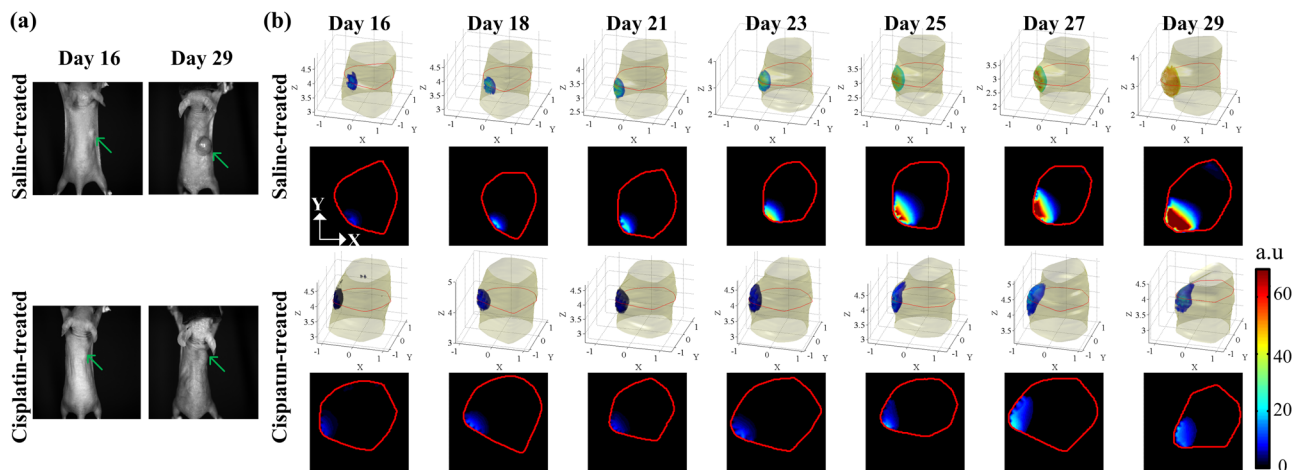


Fig. 3 Tomographic monitoring of tumor response to cisplatin *in vivo*. (a) White-light images of the saline-treated mouse and the cisplatin-treated mouse on day 16 and day 29, respectively. The green arrows indicate the location of the tumor. (b) Series of subsurface FMT reconstruction results. The first and third rows show the 3-D rendering of the reconstructed fluorescence distributions of the saline-treated mouse and the cisplatin-treated mouse, respectively. The second and fourth rows show the cross-section images of the saline-treated mouse and the cisplatin-treated mouse, respectively, taken at the center of the tumor. The red curves on the cross-section images represent the mouse boundary.

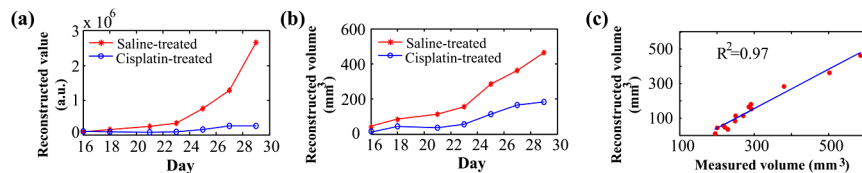


Fig. 4 Quantitative analysis of *in vivo* experiment. (a) Time dependence of the sum of reconstructed values in the tumor region. (b) Time dependence of the reconstructed tumor volumes. (c) The correlation between the reconstructed and the measured tumor volumes. Blue solid line, linear fit ($R^2 = 0.97$).

intratumorally every day for 2 consecutive weeks, while the other tumor-bearing mouse was injected with saline solution to serve as the nontreated control. To monitor the therapeutic response, subsurface FMT was conducted on days 16, 18, 21, 23, 25, 27, 29. In the *in vivo* study, fluorescent images were acquired with a 530 ± 5 nm excitation filter and a 613 ± 38 nm emission filter. Background images were acquired with a 480 ± 5 nm excitation filter for background signal reduction.¹¹ 72 white-light images were collected to recover the 3-D surface of the mouse.¹² The mice were anesthetized by isoflurane-oxygen gas mixture during the imaging process. The optical properties used in subsurface FMT reconstruction were $\mu_a = 0.8 \text{ cm}^{-1}$, $\mu'_s = 13.2 \text{ cm}^{-1}$, which were calculated according to Ref. 13. Tumors were measured with a caliper after fluorescence imaging and tumor volume was estimated based on the formula $0.5 \times a \times b^2$, where a was the longest diameter and b was the shortest diameter. The 3-D geometry of the two mice were both discretized with a voxel size of $0.2 \times 0.2 \times 0.2 \text{ mm}^3$, and the reconstructed tumor volumes were calculated by the product of voxel size and the number of voxels in the tumor region.

The white-light images of the saline-treated mouse and the cisplatin-treated mouse at the beginning and the end of the anti-tumor treatment are depicted in Fig. 3(a). Reconstruction results shown in Fig. 3(b) illustrate a difference in the growth of tumor fluorescence intensities between the two mice. Quantitative evaluation based on the sum of reconstructed values in the tumor region, as depicted in Fig. 4(a), demonstrates that the fluorescence intensity is stable in the cisplatin-treated mouse, but increases dramatically in the saline-treated control. The time dependence of reconstructed tumor volumes for both mice is shown in Fig. 4(b), and high correlation between the reconstructed and the measured tumor volumes is obtained, as shown in Fig. 4(c).

As a noninvasive technique that discovers fluorescence distribution by tomographic means in reflectance geometry, subsurface FMT is able to three-dimensionally and quantitatively image molecular and cellular activities not only on the surface but in the interior tissues, thus providing a useful tool for serial, noninvasive monitoring of therapeutic response in preclinical studies. In this work, the localization and quantification accuracy of the subsurface FMT method is validated in phantom experiments. Then the therapeutic response of cisplatin is monitored *in vivo*, and the distribution of DsRed is tracked three-dimensionally during the treatment. Future works include the application of this approach in the optimization of existing cancer treatment regimens and testing of novel therapeutic paradigms in the preclinical setting, as

well as informing the design and management of future clinical trials.

Acknowledgments

This work is supported by the National Basic Research Program of China (973) under Grant No. 2011CB707701, 2011CB707704; the National Major Scientific Instrument and Equipment Development Project under Grant No. 2011YQ030114; the National Natural Science Foundation of China under Grant No. 81071191, 60831003, 30930092, 30872633; the Beijing Natural Science Foundation Grant No. 3111003; the Tsinghua-Yue-Yuen Medical Science Foundation.

References

1. V. Ntziachristos, "Illuminating disease with fluorescence molecular tomography," *3rd IEEE International Symposium on Biomedical Imaging: Nano to Macro*, pp. 375–377 (2006).
2. M. Yang et al., "Whole-body optical imaging of green fluorescent protein-expressing tumors and metastases," *Proc. Natl. Acad. Sci. USA* **97**(3), 1206–1211 (2000).
3. H. C. Manning et al., "Molecular imaging of therapeutic response to epidermal growth factor receptor blockade in colorectal cancer," *Clin. Cancer Res.* **14**(22), 7413–7422 (2008).
4. Z. Medarova et al., "Multiparametric monitoring of tumor response to chemotherapy by noninvasive imaging," *Cancer Res.* **69**(3), 1182–1189 (2009).
5. F. Leblond et al., "Pre-clinical whole-body fluorescence imaging: review of instruments, methods and applications," *J. Photochem. Photobiol. B.* **98**(1), 77–94 (2010).
6. V. Ntziachristos, "Fluorescence molecular imaging," *Annu. Rev. Biomed. Eng.* **8**, 1–33 (2006).
7. D. Kepshire et al., "Fluorescence tomography characterization for subsurface imaging with protoporphyrin IX," *Opt. Exp.* **16**(12), 8581–8593 (2008).
8. S. Bjorn et al., "Reconstruction of fluorescence distribution hidden in biological tissue using mesoscopic epifluorescence tomography," *J. Biomed. Opt.* **16**(4), 046005 (2011).
9. A. D. Klose and E. W. Larsen, "Light transport in biological tissue based on the simplified spherical harmonics equations," *J. Comput. Phys.* **220**(1), 441–470 (2006).
10. D. F. Wang, X. Liu, and J. Bai, "Analysis of fast full angle fluorescence diffuse optical tomography with beam-forming illumination," *Opt. Exp.* **17**(24), 21376–21395 (2009).
11. N. C. Deliolanis et al., "In vivo tomographic imaging of red-shifted fluorescent proteins," *Biomed. Opt. Exp.* **2**(4), 887–900 (2011).
12. D. F. Wang et al., "In-vivo fluorescence molecular tomography based on optimal small animal surface reconstruction," *Chin. Opt. Lett.* **8**(1), 82–85 (2010).
13. G. Alexandrakis, F. R. Rannou, and A. F. Chatzioannou, "Tomographic bioluminescence imaging by use of a combined optical-PET (OPET) system: a computer simulation feasibility study," *Phys. Med. Biol.* **50**(17), 4225–4241 (2005).